

# **Synergistic Regulation of Border Cell Migration by *Singed* and Arp2/3 Complex in *Drosophila*: Insights into F-Actin Dynamics**

A Thesis

submitted to

Indian Institute of Science Education and Research Pune in partial  
fulfillment of the requirements for the BS-MS Dual Degree Programme

By

Netra Pegu



Indian Institute of Science Education and Research Pune Dr.  
Homi Bhabha Road,  
Pashan, Pune 411008, INDIA.

Date: April, 2024

Under the guidance of

Supervisor: Dr. Pralay Majumder

Assistant Professor, Presidency University

From May 2023 to March 2024

INDIAN INSTITUTE OF SCIENCE EDUCATION AND RESEARCH PUNE

# Certificate

This is to certify that this dissertation entitled “**Synergistic Regulation of Border Cell Migration by *Singed* and Arp2/3 Complex in *Drosophila*: Insights into F-Actin Dynamics**” towards the partial fulfillment of the BS-MS dual degree programme at the Indian Institute of Science Education and Research, Pune, represents study/work carried out by Netra Pegu at Indian Institute of Science Education and Research under the supervision of Dr. Pralay Majumder, Assistant Professor, Department of Life Sciences, Presidency University, Kolkata during the academic year 2023-2024.



Dr. Pralay Majumder

Dr. Pralay Majumder  
Assistant Professor (Biological Sciences)  
PRESIDENCY UNIVERSITY, KOLKATA

Committee: Biology

Dr. Pralay Majumder

TAC: Dr. Gayathri Pananghat

# Dedication

This dissertation work is dedicated to my loving family, whose unwavering support and encouragement have been the cornerstone of my academic journey. I am grateful for their sacrifices, understanding, and belief in my abilities, which have inspired me to pursue excellence in every endeavor.

I also dedicate this work to my supervisor, Dr. Pralay Majumder, lab mentors, and educators, whose guidance and wisdom have shaped my thinking during the whole process of my dissertation work and contributed significantly to my growth as a researcher. Their invaluable feedback and constructive criticism have challenged me to push boundaries and strive for innovation in my research.

Finally, I dedicate this paper to all those who seek knowledge and truth, hoping that the findings presented here may contribute positively to the advancement of science and benefit society as a whole.

# Declaration

I hereby declare that the matter embodied in the report entitled “**Synergistic Regulation of Border Cell Migration by *Singed* and Arp2/3 Complex in *Drosophila*: Insights into F-Actin Dynamics**” are the results of the work carried out by me at the Fly Lab, Department of Life Sciences, Presidency University, Kolkata, under the supervision of Dr. Pralay Majumder and the same has not been submitted elsewhere for any other degree.



Netra Pegu

Date: 15/04/2024

# Acknowledgment

I am immensely grateful to Dr. Pralay Majumder, my esteemed supervisor from the Presidency University (Department of Life Sciences), Kolkata, for entrusting me with this invaluable research opportunity and guiding me diligently throughout the entire research process. His expertise and unwavering support have been instrumental in shaping this work.

I extend my heartfelt gratitude to my expert advisor, Dr. Gayathri Pananghat from IISER Pune, for her invaluable guidance and mentorship. Her insights and encouragement have significantly contributed to the success of this project.

I would also like to express my sincere appreciation to Mr. Sandipan Mukherjee, Ms. Poulami Chatterjee, Mr. Sayantan Dutta, and Mr. Shroyon Sarkar, all esteemed Ph.D. students, and the entire Fly Lab group at Presidency University for their unwavering support, insightful discussions, and valuable guidance during my thesis work. Their collective expertise and encouragement have been invaluable in navigating the complexities of this research.

Furthermore, I extend my gratitude to IISER Pune for providing me with the opportunity to work on my master's project, which has been a rewarding and enriching experience.

# Table of Contents

## List of Tables

Table 1: Reagents, Manufacturer and Catalogue Number .....	18
Table 2: Stock Number, Genotypes, and Source.....	19
Table 3: RNAi names and the genotypes of F1 in genetic screening .....	21

## List of Figures

Figure 1: Protrusion showing lamellipodia and filopodia .....	12
Figure 2: Representative figure showing the path of BC migration .....	24
Figure 3: Genetic interaction between <i>singed</i> and <i>arp2/3</i> complex during border cell migration.....	28
Figure 4: <i>singed</i> and <i>arp2/3</i> complex regulates F-actin density in BCs during border cell migration .....	30
Figure 5: <i>singed</i> and <i>arp2/3</i> complex affects border cell morphology in fixed samples .....	31
Figure 6: Representative image of F1 flies for <i>hs&gt;FLP; AY-GAL4, 17b, UAS&gt;RedStingernIs6/TM3, Sb</i> flies .....	33
Figure 7: Representative image of F1 flies for <i>hs&gt;FLP/singed; AY-Gal4, 17b, UAS&gt;RedStingernIs6/arp2</i> flies .....	34

## Chapters:

<b>Abstract .....</b>	<b>9</b>
<b>Introduction.....</b>	<b>9</b>
Cell Migration .....	9
Lamellipodia and Filopodia .....	12
Role of <i>Arp</i> complex, WAVE and elongating factors.....	13
Role of formins, parallel bundle cross-linkers and small GTPases .....	14
<b>Materials and Methods .....</b>	<b>18</b>
<i>Drosophila</i> stocks and strains.....	19

Crossing schemes .....	20
Dissection and Immunostaining .....	22
Counting of BC migration defect .....	23
Quantification of total F-actin in BC cluster from fixed imaging .....	24
Determination of BC cluster phenotype from fixed imaging .....	26
Figures, graphs, and statistical analysis .....	26
<b>Results .....</b>	<b>27</b>
Cluster shape from fixed imaging .....	31
<b>Discussion.....</b>	<b>34</b>
Significance of the study.....	36
<b>References .....</b>	<b>37</b>



## **Abstract**

Stages 8, 9, and 10 of *Drosophila* oogenesis are critical for border cell (BC) migration. During stage 8, migration initiation occurs, while stage 9 sees BCs traversing nurse cells toward the oocyte. By stage 10, BCs reach the oocyte, necessitating close contact. In collective cell migration (CCM), the leading cells in the cohort generate forward protrusions, and lagging cells make backward retractions in a harmonized and concerted manner. Effectively, the actin cytoskeleton stands as the leading driver of protrusion formation and retractions.

Using *Drosophila melanogaster* as a model, we study collective cell migration (CCM) in border cells (BCs). *Singed* (the vertebrate homolog of *fascin*) and the Arp2/3 complex genetically interact to regulate F-actin architecture in BCs. Depletion of both hindered migrations, leading to a substantial cell migration defect. Both collaborate to regulate F-actin density in border cell clusters. The consequence of F-actin alteration is manifested upon cluster shape and area as clusters become large and rounded. As the BC cluster's shape depends on mechanical and physiological behavior of the individual border cell, we can predict a relationship between shape increase and border cell number. Our experiment focuses on three signaling pathways governing migration: a global steroid-hormone signal coordinating migration timing, a localized cytokine signal activating the Jak-Stat pathway for migration induction, and a growth factor guiding cells to their destination.

We have made an experimental setup to observe each of the individual cells of the cluster and count their number through fixed imaging for both control and double knockdown. Furthermore, we are trying to find the correlation of *stat92E* and *slbo* with *singed* and *arp2* during border cell migrations through genetic interaction studies.

## **1. Introduction**

### **1.1. Cell Migration:**

“Cell migration is an important process that is involved in the major developmental stages

of all complex organisms and results in the arrangement of cells into a precise architecture, the organization of the nervous system, and the generation of specialized organs and tissues” [1].

Cell migration is a compelling and multifaceted phenomenon, comprising both single-cell and collective-cell dynamics. Single-cell migration involves the movement of individual cells, while collective-cell migration represents a synchronized effort among multicellular assemblies, orchestrated through intricate mechanical and chemical interactions [40]. The collective migration of cells introduces a heightened level of fascination and complexity, as it entails the coordinated movement of cell cohorts or sheets, signifying a profound orchestration of biological processes.

This collective cellular endeavor holds paramount significance in various physiological contexts, including embryonic organogenesis, wound healing, immune responses, and tissue homeostasis [2,3]. Within the realm of embryonic development, collective cell migration plays a pivotal role in establishing the intricate morphogenetic architecture essential for proper organ formation and function [38]. Moreover, the concerted migration of cells contributes significantly to the dynamic processes of tissue repair, immune surveillance, and maintenance of tissue equilibrium.

An exemplary manifestation of CCM unfolds in the context of BCM within the *Drosophila melanogaster* fruit fly model system. The *Drosophila* egg chamber emerges as an invaluable experimental platform for dissecting the molecular and cellular underpinnings of collective cell migration, owing to its inherent accessibility and genetic tractability. Through the lens of this model organism, researchers gain profound insights into the regulatory mechanisms governing the coordinated movement of cell populations, unraveling fundamental principles underlying tissue morphogenesis and homeostasis.

For our experiment, we will use one of the elegant models of collective cell migration called border cell (BC) migration in the genetically tractable model system *Drosophila*

*melanogaster*. *Drosophila* egg chamber consists of one oocyte and 15 nurse cells of germ-line origin, enclosed by a single layer of about 700 somatic follicle cells (FC) [39]. About 4-8 anterior FC form migratory BC that migrates about 150 $\mu$ m toward the oocyte. This BC migration is cohort-type collective cell migration, which requires JAK-STAT to specify and maintain the cohort, ecdysone to define timing, RTKs for guidance, and actin cytoskeleton for protrusion [3].

Various mutants display atypical protrusions, yet the exact mechanism behind their formation remains to be investigated. The BC cluster operates as a resilient process with inherent redundancies. Within the protrusions of the cluster, actin-interacting proteins orchestrate a consistent and iterative turnover of F-actin filaments, driving spatial and temporal remodeling of the actin cytoskeleton during migration. Consequently, this process induces notable morphological alterations within the cluster and dynamic protrusions, ultimately defining the cluster's motility capacity [4, 5]. Therefore, we would like to unravel the mechanism behind protrusion formation in BCs, shedding light on the diverse facets of protrusion morphology.

Cell migration can be delineated into three sequential phases: protrusion, characterized by the extension of an actin-rich membrane at the leading edge, which senses guidance cues; anchoring, involving the attachment of adhesion molecules within migrating cells to the external environment; and retraction of the trailing edge, primarily facilitated by myosin II-driven actin depolymerization, propelling the cells forward [6,7]. Our primary focus will be on protrusion, characterized by dynamic plasma membrane extensions such as sheet-like lamellipodia or finger-like filopodia, whose formation relies on the actin cytoskeleton. Migrating cells exhibit spontaneous switching between protrusions, with the selection between lamellipodia and filopodia determined by the interplay among actin polymerization, contraction, and adhesion [4].

## 1.2. Lamellipodia and Filopodia

Lamellipodia are typically characterized as 'mesenchymal' structures and are orchestrated by the Arp2/3 and SCAR/WAVE (Suppressor of cAMP Receptor/WASP-family Verprolin-homologous protein) complexes under the guidance of Rac. In contrast, filopodia are primarily regulated by formins and VASP while being stabilized by actin cross-linkers like singed [5]. Filopodia may or may not involve the SCAR/WAVE and

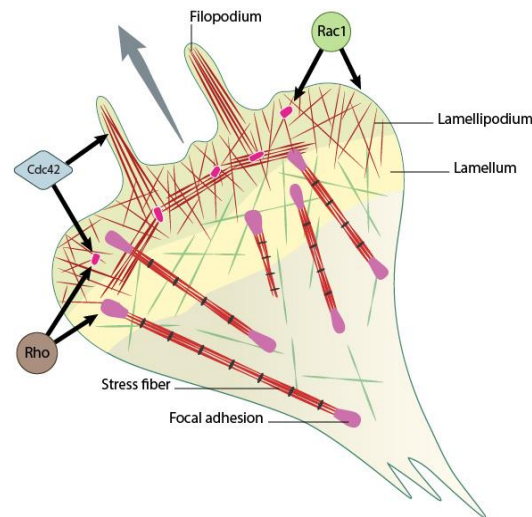


Fig. 1. **Protrusion showing lamellipodia and filopodia**

Source: MBI, NUS.

<https://www.mbi.nus.edu.sg/mbinfo/what-is-the-role-of-rho-gtpases-in-the-regulation-of-focal-adhesion-assembly/>

WASP complexes, yet they are known to contain fascin (the *Drosophila* homolog of singed) and crosslinking proteins that stabilize parallel F-actin arrangements [8,9].

Border cells engage in protrusion formation during migration, which has been identified as predominantly lamellipodial in nature [10]. Despite expressing singed at high levels, the absence of singed in border cells does not impact their migratory capability [11]. We hypothesized that the expression of singed, being a significant cellular energy investment, must play a role in border cell migration, albeit potentially redundant. To verify our

hypothesis, we will conduct a genetic screening of actin binding proteins that affects the BC migration.

The actin cytoskeleton, a vital component within cells, functions as the primary force-generating apparatus. Actin filaments typically exhibit polarity, characterized by a rapidly polymerizing barbed end and a slower-growing (depolymerizing) pointed end [41]. Protrusions occur as monomeric G-actin polymerizes just beneath the plasma membrane, forming F-actin structures. In cellular dynamics, two predominant choices emerge: (i) branched filaments and (ii) long parallel or bundled filaments. Branched filaments are instrumental in forming lamellipodial protrusions, which contribute to cell motility and shape changes. Conversely, long parallel or bundled filaments facilitate the formation of filopodial protrusions, aiding in cell adhesion and signaling processes. Initiating or nucleating either filament type presents a challenge, yet once initiated, filaments can undergo self-sustained growth, contributing to diverse cellular functions and structural integrity.

### **1.3. Role of Arp complex, WAVE and elongating factors:**

Branching predominantly occurs through the action of a pivotal actin-branching, seven-member actin related protein complex Arp2/3. This complex is activated by nucleation-promoting factors (NPFs) such as Wiskott-Aldrich syndrome Protein (WASP) and WASP and Verprolin homologous protein (SCAR/WAVE) [12, 13]. WASP and Scar/WAVE proteins emerge as pivotal orchestrators of the actin cytoskeleton, wielding profound influence through their versatile domains. Among their shared attributes, the VCA domain stands out as a potent activator of the Arp2/3 complex [42], comprising the V domain, which binds to G-actin monomers, and the CA domain, which interacts intricately with the Arp2/3 complex [34]. This collective functionality renders the VCA domain a compelling catalyst for Arp2/3 complex activation, pivotal in driving actin polymerization and cytoskeletal dynamics [35].

The WASP and WAVE family proteins serve as indispensable guardians of actin dynamics, steering cellular processes through their multifaceted interactions. The recognition of the Cdc42-Rac-interactive binding (CRIB) domain within WASP underscores its intricate involvement in signaling cascades, notably through its association with p21-activated kinase (PAK) homology domains [36]. Thus, both WAVE and WASP regulate Arp2/3-mediated F-actin branching and increase the free barbed ends [13].

Notably, studies have illuminated the nuanced interplay between WAVE and WASP proteins in shaping cellular morphology and motility dynamics. Knockdown (KD) of WAVE proteins has been shown to perturb lamellipodia formation while concurrently stimulating the emergence of filopodia structures, indicative of their role in lamellipodial dynamics [38]. Intriguingly, simultaneous KD of both WAVE and WASP proteins leads to a synergistic augmentation of filopodia formation, underscoring the intricacies of their collaborative and compensatory mechanisms in regulating cytoskeletal architecture and cellular motility [25].

In essence, the dynamic interplay between WASP and Scar/WAVE proteins serves as a cornerstone in the orchestration of actin cytoskeletal dynamics, underscoring their indispensable roles in cellular physiology and morphogenesis. Through their multifunctional domains and intricate regulatory mechanisms, these proteins govern fundamental processes essential for cellular homeostasis and function.

#### **1.4. Role of formins, parallel bundle cross-linkers and small GTPases:**

The orchestration of cellular motility and structural integrity hinges upon a finely tuned interplay of various proteins within the actin cytoskeleton. At the heart of this intricate network, cross-linkers such as alpha-actinin and filamin emerge as central players, diligently holding together branched actin filaments within the cellular framework. Their collaborative efforts establish the structural scaffolding necessary for cellular movement and shape maintenance.

Amidst this dynamic milieu, proteins like cortactin take center stage by binding to the elongating barbed ends of actin filaments, thereby bolstering their stability and resilience. Concurrently, elongating factors such as Ena localize at the lamellipodial tip, where they actively foster the elongation of Arp-dependent actin branching filaments, perpetuating cellular protrusions crucial for motility and exploration.

Following a phase of elongation, the delicate balance of actin dynamics is meticulously regulated by proteins like CapZ, which cap the barbed ends of filaments when necessary, ensuring optimal network length and integrity. Complementing this rapid polymerization, profilin facilitates swift actin polymerization, while the nuanced process of depolymerization at blunt ends is facilitated by actin-severing proteins like ADF/Cofilin, ensuring controlled turnover and remodeling [12, 13, 14, 15].

Moreover, the class of formin variants, exemplified by FMNL2 and FMNL3, emerges as pivotal contributors to actin dynamics, particularly at the lamellipodial tip. Here, they spearhead the elongation of Arp-dependent actin branching filaments, amplifying cellular protrusions and facilitating directional migration [12, 14, 15].

Recent insights have unveiled the nucleating prowess of specific formins such as mDia2 in lamellipodia, where formin-nucleated filaments serve as primordial templates for Arp2/3-mediated nucleation, further highlighting the intricacies of actin cytoskeleton regulation in cellular motility and structural plasticity [32,33]. Thus, through a choreographed symphony of molecular interactions, the actin cytoskeleton orchestrates cellular dynamics essential for physiological processes ranging from migration to tissue morphogenesis.

Vertebrate Arp2/3(220 kDa) complex comprises Arp2 and Arp3 as two core subunits forming the first two subunits of the daughter filament [16, 17]. The dimer composed of ARPC2 and ARPC4 serves as the structural core of the complex, facilitating interaction with the template filament [18, 19, 20]. ARPC3 acts as a bridge between Arp3 and the mother filament, while ARPC5 facilitates the binding of Arp2 to the rest of the complex [19]. ARPC1 plays a crucial role in binding Nucleation Promoting Factors (NPFs) to the complex [20]. Studies indicate that phosphorylation of Arp2 is essential for the Arp2/3

complex to bind to actin filament barbed ends and initiate nucleation in cultured *Drosophila* cells [21].

F-actin fibers nucleated by formins typically organize into parallel bundles, stabilized by cross-linking proteins such as fascin, fimbrin, and villin. Ena proteins contribute to the elongation of actin bundles at their growing tips [22, 23]. Additionally, certain formins themselves may function as cross-linkers in this process [24]. The chief supreme Rho GTPases, such as Rho, Rac1, and Cdc42, exert significant control over crucial participants in actin-based cellular structures, particularly during the process of cell migration. Their activity oscillates between the inactive GDP form and the active GTP form, a transition facilitated by GTPase Activating Proteins (GAPs) and Guanine Exchange Factors (GEFs), respectively. Rac1 is responsible for promoting the formation of Arp2/3-mediated branched actin filaments, while Cdc42 typically initiates branching of F-actin through formins. Moreover, Cdc42 plays a crucial role in recruiting WASP for Arp2/3-mediated branching [13, 14].

Examining the existing pathways reveals that ROCK stands out as a prominent target of Rho GTPase [24], while Nucleation Promoting Factors (NPFs) such as WASP consistently bind to Cdc42 rather than Rac1 GTPase [25, 26]. Rac1 GTPase has been found to activate WAVE [5]. Specific protrusions rely on NPFs like WASP and WAVE for Arp2/3-mediated branching [4]. Therefore, it can be inferred that the activity of the Arp2/3 complex is contingent upon both Rac1 and Cdc42 GTPases, rather than Rho/ROCK.

It has been observed that Cdc42-mediated activation of WASP activates fascin [27, 28]. Moreover, under the influence of WASP and Rac1, formins can nucleate branched F-actins [27, 28]. We have also seen that variants like FMNL2 and FMNL3 primarily regulate the tips of parallel F-actin bundles, and they also possess the capability to elongate branched actin filaments [29, 30]. Consequently, there exists a genetic crosstalk among actin-interacting proteins within protrusions of migrating cells. Given the actin-rich nature of BC clusters, such crosstalk is anticipated to be prominently evident.

In *Drosophila*, a variety of vertebrate homologs of proteins conducive to protrusion dynamics, such as chickadee, human profilin homolog, the *formin* family

protein Dia, cheerio, mammalian homolog filamin, etc., actively facilitate BC migration. Notably, *singed* (*Fascin* homolog) shows high expression levels without discernible effects on BC migration [11]. While the Arp2/3 complex assumes diverse roles in blastoderm organization, eye morphogenesis, axon development, bristle formation, growth of ring canals, and nurse cell cytoplasm dumping, etc., evidence regarding its role in proper protrusion characterization remains lacking.

The 57kDa *Fascin*, akin to *Drosophila*'s homolog *Singed*, exhibits heightened expression levels within BCs [11], making it a pivotal marker for tracking BC migration. In vertebrates, *Fascin* assumes multifaceted roles within actin-based structures. Beyond its conventional role as the principal cross-linker for parallel actin bundles in migrating cell protrusions, it is also implicated in fostering the formation of branched actin networks in various migrating cells [27]. Conversely, in *Drosophila*, *singed* orchestrates a spectrum of functions, spanning from facilitating nurse cell dumping to orchestrating the assembly of parallel bundles in bristles, and maintaining nuclear architecture [11, 27, 31].

Given the diverse roles exhibited by *Singed* in *Drosophila* and *Fascin* in vertebrates, it's plausible to anticipate a degree of redundancy in their functions within border cells. Unveiling this redundancy necessitates comprehensive genetic interaction studies between *Singed* and an array of actin-interacting proteins within BCs. Consequently, it's reasonable to hypothesize that the Arp2/3 complex and *Singed* may engage in genetic interactions, jointly regulating F-actin dynamics to finely orchestrate the characteristic protrusion dynamics in BCs.

As such, the exploration of genetic screening studies holds promise in uncovering an intricate signaling pathway that underlies the orchestrated migration of border cells, elucidating the nuanced interplay between *Singed*, the Arp2/3 complex, and a myriad of actin-interacting proteins.

## **2. Materials and Methods:**

**Table 1: Reagents, Manufacturer and Catalogue Number**

<b><u>Reagent</u></b>	<b><u>Manufacturer</u></b>	<b><u>Cat-No</u></b>
S2 Media	HIMEDIA	IML003
FBS	HIMEDIA	RM 1112
Insulin	SRL	31773
Formaldehyde	SIGMA	252549
PBS, pH-7.4	HIMEDIA	TL1099
1 M Tris-HCl, pH 7.4	HIMEDIA	ML028
150 mM NaCl	SRL	7647-14-5
1% IGEPAL	M P Biomedical	CA-630
BSA	SRL	9048-46-8
90% Glycerol Anhydrous	SRL	56-81-5
0.5% N-Propyl Gallate	SRL	121-79-9
Rat anti-DE-cadherin	DSHB	1:10 (DCAD2)
mouse anti-Fasciclin III	DSHB	1:25 (Fas3; 7G10)
mouse anti-Fascin	DSHB	1:10 (Sn7C)
mouse anti-armadillo	DSHB	1:100 (N2 7A1)
anti-beta tubulin antibody	DSHB	1:20 (E7)
rabbit anti-GFP	Abcam	1:2000 (ab 6556)

Alexa Fluor 488 anti-mouse	Abcam	1:800 (ab 150117)
Alexa Fluor 568 anti-mouse	Abcam	1:800 (ab 175700)
Alexa Fluor 488 anti-rat	Abcam	1:800 (ab 150165)
DAPI (0.05 µg/ml)	Molecular Probes	D1306
Phalloidin coupled with Alexa Fluor 568	Life Technologies	A12379

## 2.1. Drosophila stocks and strains:

For our experiments, we have used *c306-GAL4*, *tubP-GAL80<sup>ts9</sup>* driver for all our RNAi-mediated screening and gene over-expression experiments. These drivers offer precise control over gene expression in *Drosophila melanogaster*, enabling targeted manipulations within specific tissue contexts. Key to our genetic manipulations have been the UAS-RNAi constructs, primarily obtained from the Bloomington *Drosophila* Stock Center (BDSC), otherwise stated. Notably, constructs #42615 and #27705 from BDSC have been instrumental in our investigations, particularly for knockdown experiments targeting *singed* and *arp2* genes respectively.

**Table 2: Stock Number, Genotypes and Source**

<u>Stock number</u>	<u>Genotype</u>	<u>Source</u>
57805	<i>sn</i> RNAI(II)	BDSC
42615	<i>sn</i> RNAI(III)	BDSC

<b>27705</b>	<i>arp2</i> RNAi	BDSC
<b>27044</b>	<i>arpc3a</i> RNAi	BDSC
<b>53972</b>	<i>arp3</i> RNAi	BDSC
<b>28720</b>	<i>arpc5</i> RNAi	BDSC
<b>42875</b>	<i>arpc4</i> RNAi	BDSC
<b>31246</b>	<i>arpc1</i> RNAi	BDSC
<b>62339</b>	<i>arpc2</i> RNAi	BDSC
	<i>Hs&gt;FLP; AY-GAL4, 17b, UAS&gt;RedStingernls6/TM 3, Sb</i>	Dr. Jocelyn McDonald (Kansas State University)

### **3.2. Crossing schemes:**

In our RNA interference (RNAi) experiments, crosses were meticulously established at a temperature of 18°C. The modulation of gene expression via UAS-RNAi and UAS-overexpression constructs was achieved by harnessing the regulatory prowess of the *c306-GAL4*, *tubP-GAL80<sup>ts9</sup>* drivers, strategically deployed within the border cells. 10 days old F1 flies from 18°C crosses were then fattened (forced to eat more dry yeast) at 30°C for 16 h before we performed dissection. In the case of live imaging, fattening was done for 13 h prior to dissection. All the genotypes of the F1 flies for all the experiments have been mentioned in table below.

**Table 3: RNAi names and the genotypes of F1 in genetic screening**

RNAi name in figures	The genotypes of F1 in genetic screening
control	<i>c306-GAL4, tubP-GAL80<sup>ts9</sup>/+, +/+</i>
<i>sn</i>	<i>c306-GAL4, tubP-GAL80<sup>ts9</sup> /+; +/+; UAS-singed RNAi/+</i>
<i>arp2</i>	<i>c306-GAL4, tubP-GAL80<sup>ts9</sup> /+; +/+; UAS-arp2 RNAi/+</i>
<i>arpc5</i>	<i>c306-GAL4, tubP-GAL80<sup>ts9</sup> /+; +/+; UAS-arpc5 RNAi/+</i>
<i>arpc4</i>	<i>c306-GAL4, tubP-GAL80<sup>ts9</sup> /+; +/+; UAS-arpc4 RNAi/+</i>
<i>arpc2</i>	<i>c306-GAL4, tubP-GAL80<sup>ts9</sup> /+; +/+; UAS-arpc2 RNAi/+</i>
<i>arpc3a</i>	<i>c306-GAL4, tubP-GAL80<sup>ts9</sup> /+; +/+; UAS-arpc3a RNAi/+</i>
<i>arp3</i>	<i>c306-GAL4, tubP-GAL80<sup>ts9</sup> /+; +/+; UAS-arp3 RNAi/+</i>
<i>arpc1</i>	<i>c306-GAL4, tubP-GAL80<sup>ts9</sup> /+; +/+; UAS-arpc1 RNAi/+</i>
<i>sn+arp2</i>	<i>c306-GAL4, tubP-GAL80<sup>ts9</sup> /+; +/+; UAS-singed RNAi/ UAS-arp2 RNAi</i>
<i>sn+arpc5</i>	<i>c306-GAL4, tubP-GAL80<sup>ts9</sup> /+; +/+; UAS-singed RNAi/ UAS-arpc5 RNAi</i>
<i>sn+arpc4</i>	<i>c306-GAL4, tubP-GAL80<sup>ts9</sup> /+; +/+; UAS-singed RNAi/ UAS-arpc4 RNAi</i>
<i>sn+arpc2</i>	<i>c306-GAL4, tubP-GAL80<sup>ts9</sup> /+; +/+; UAS-singed RNAi/ UAS-arpc2 RNAi</i>
<i>sn+arpc3a</i>	<i>c306-GAL4, tubP-GAL80<sup>ts9</sup> /+; +/+; UAS-singed RNAi/ UAS-arpc3a RNAi</i>

<i>sn+arp3</i>	<i>c306-GAL4, tubP-GAL80<sup>ts9</sup> /+; +/+; UAS-singed RNAi/ UAS-arp3 RNAi</i>
<i>sn+arpc1</i>	<i>c306-GAL4, tubP-GAL80<sup>ts9</sup> /+; +/+; UAS-singed RNAi/ UAS-arpc1 RNAi</i>

For *hs>FLP; AY-GAL4, 17b, UAS>RedStingernls6/TM3, Sb*, the experiment was done by setting up crosses at 25°C. F1 flies from 25°C crosses were then given heat shock (HS) at 37°C followed by recovery time. The time for heat shock was 1 hour followed by 5-hour recovery time and then 1 hour HS again, followed by 3-day recovery time and then fattened (forced to eat more dry yeast) at 30°C for 14 h prior to dissection.

### **3.3. Dissection and Immunostaining:**

The immunostaining protocol employed in this study closely adhered to the methodology outlined in Majumder et al, 2012[3]. Specifically, for assessing border cell migration (BCM) defects, intact ovaries sourced from 5- to 6-day-old female *Drosophila* flies were meticulously dissected using a coarse dissection approach in Schneider's Insect media. This dissection medium was supplemented with 10% fetal bovine serum (FBS) and 0.20 mg/ml insulin to ensure optimal conditions for tissue preservation. Subsequently, the dissected ovaries were promptly fixed in a 4% formaldehyde solution prepared in 1X phosphate buffer saline (PBS) with a pH of 7.4, a process that lasted for 10 minutes.

Following fixation, the fixed ovaries underwent a series of rinses in NP40 buffer (composed of 50 mM Tris-HCl, pH 7.4, 150 mM NaCl, 1% IGEPAL, and 5 mg/ml bovine serum albumin (BSA)) to remove any residual fixative and prepare them for antibody incubation. The ovaries were then incubated overnight at 4°C with primary antibodies, carefully optimized to specific dilutions (see Table 1 for details). The subsequent day, excess primary antibodies were thoroughly washed off through rapid NP40 buffer rinses, accompanied by a 2-hour washing step.

Following primary antibody removal, the fixed ovaries were subjected to secondary antibody incubation (as per Table 1) along with DAPI staining for nuclear visualization, a process lasting 2 hours at room temperature. Excessive secondary antibodies were subsequently removed through quick NP40 buffer washes, followed by a 2-hour washing step. The individual egg chambers were then separated from the ovaries via rapid pipetting and mounted onto slides using a mounting medium comprising 90% Glycerol Anhydrous, 0.5% N-Propyl Gallate, and 20 mM Tris-HCl (pH 7.4).

### **3.4. Counting of BC migration defect:**

The immuno-stained and fixed egg chambers were meticulously observed using the Zeiss Axio Lab. A1 epifluorescence microscope to assess the percentage migration defect during genetic interaction analyses. We conducted a thorough assessment of the migration route traversed by the border cell (BC) cluster, extending from the egg chamber's anterior tip to the oocyte's anterior margin, which was regarded as 100% migration. Any failure of the BC cluster to reach the oocyte's anterior margin was deemed a migration defect. Typically, full migration of the BC cluster is attained by stage 10 of development; therefore, we focused specifically on stage 10 egg chambers for this analysis.

The assessment of migration completion was predicated upon the positioning of the BC cluster within the egg chamber. If the BC cluster resided anywhere within the 75% zone of the migration pathway, the migration was deemed incomplete. Conversely, if the BC clusters had migrated beyond the 75% zone, indicating complete migration, it was categorized as 100% migration (refer to Fig 2 for visualization).

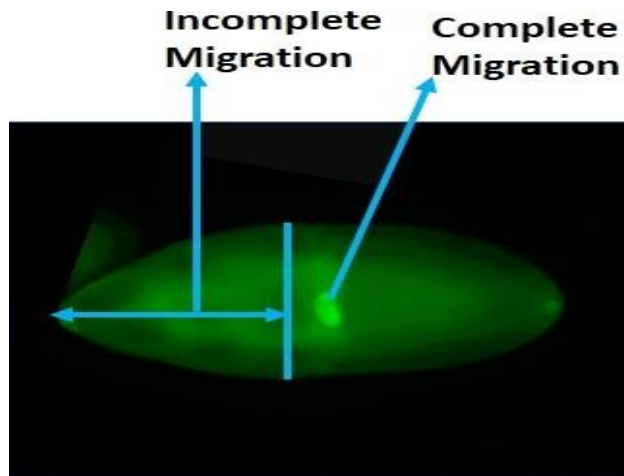


Fig. 2. Representative figure showing the path of BC migration

For the calculation of migration defect, the following formula was applied:

**Percentage of Incomplete Migration** = (Number of Stage 10 egg chambers with incomplete BC migration / Total number of Stage 10 egg chambers) x 100.

This meticulous methodology allowed for a precise and quantitative assessment of BC migration defects, enabling a deeper understanding of the genetic interactions governing this crucial developmental process.

### **3.5. Quantification of total F-actin in BC cluster from fixed imaging**

In our examination of F-actin intensity within border cell (BC) clusters, we embarked on a rigorous staining and imaging protocol utilizing fixed egg chambers from various genetic backgrounds. We examined control samples, *tubP-GAL80<sup>ts9</sup>* mediated single knockdown of *singed* and *arp2*, as well as the double knockdown (*sn + arp2*) flies. The staining regimen involved mouse anti-armadillo followed by secondary anti-mouse 488, Phalloidin 568, and DAPI, using the reagents detailed in Table 1. These samples were then imaged using a Leica DMI8 epifluorescence microscope with a 10X objective (NA 0.3).

Each stage of the imaging procedure was meticulously carried out, including a thorough washing step designed to eliminate any unbound phalloidin and anti-armadillo, ensuring the accuracy of our findings. We meticulously applied identical camera exposure and gain settings to each channel across all egg chambers to maintain uniformity. The fluorescence intensity of the anti-armadillo acted as a reliable internal control for each egg chamber, facilitating precise comparative analysis.

The captured images were then processed using Fiji software to quantify the fluorescence intensity specifically bound to F-actin within the BC clusters. To calculate the mean pixel intensity, we initially outlined the area of BC clusters by drawing a circle around them. We then measured the background fluorescence intensity by positioning the same circle in a region encompassing the nurse cell cytoplasm. Subsequently, we subtracted the background signal from the signal derived from the BC cluster, and a relative fluorescence intensity (RFI) was computed by dividing the Alexa 488 (Phalloidin) signal by the Alexa 568 (armadillo) signal.

**Relative Fluorescence Intensity (RFI) is calculated as follows:**

$$RFI = \frac{\text{Mean intensity of armadillo (Mean intensity of border cell cluster - Mean intensity of background)}}{\text{Mean intensity of Phalloidin (Mean intensity of border cell cluster - Mean intensity of background)}}$$

The distribution of this relative fluorescence intensity was effectively depicted through a box-whisker plot, allowing for a visual representation of the data. Furthermore, we calculated the relative fold change with respect to the control, providing insights into the magnitude of changes observed in F-actin intensity across different genetic backgrounds.

### **3.6. Determination of BC cluster phenotype from fixed imaging:**

In the case of fixed imaging, we analyzed the images of all four genotypes, already captured during F-actin quantification by phalloidin having anti-arm as an internal control (already mentioned above). From these images, we determine the area, length, and width of the BC cluster. Whole border cell cluster areas were measured using Fiji software. With the help of freehand selections in Fiji software, a line was drawn along the periphery of each cluster, not considering the protrusions, to measure the cluster area. The cluster length was assessed using Fiji by drawing the longest straight line from the posterior to the anterior end of each cluster, while excluding protrusions. Additionally, cluster width was measured by drawing the longest straight line perpendicular to the anteroposterior axis of the cluster. These measurements were then visualized using box and whisker plots for each sample.

### **3.7. Graphs, figures, and statistical analysis:**

Figures underwent processing in Adobe Photoshop CC 2017 and were exported as .tif files via LasX software. Graphs were crafted using Microsoft Excel 2019. Statistical analyses were performed utilizing 'one-way ANOVA' and paired 't-test' in Microsoft Excel 2019. Significant p-values are provided in the figure legends, while nonsignificant values are omitted.

## 4. Results:

Using a genetic interaction approach, our research endeavors to unravel the intricate functions of genes governing border cell migration (BCM) in *Drosophila melanogaster*. This methodology allows us to delve into the intricate interplay between genes, unveiling how multiple genetic factors influence the manifestation of a single phenotype, such as BCM, and how they might mutually regulate each other's activities.

In our investigations, we scrutinize the scenario where the knockdown of individual genes leads to BCM defects, and explore how their simultaneous knockdown could exacerbate these defects, indicating genetic interaction. Specifically, if the combined knockdown results in a migration defect greater than the sum of the defects observed in individual knockdowns, it suggests a synergistic interaction. Conversely, if the defect remains largely similar to the cumulative effect of individual knockdowns, it implies an additive interaction.

Remarkably, our observations in the *Drosophila* ovary unveiled an intriguing aspect regarding the gene *Singed*, which exhibits heightened expression specifically in border cells (BCs). This selective expression pattern is peculiar, given that most follicle cells lack significant *Singed* expression. Surprisingly, despite its prominence in BCs, the loss of *Singed* alone does not elicit BCM defects. So, we postulated that *Singed* should be essential for BCM and hence, we raise our first question; whether *singed* can be somewhat a redundant protagonist in BCM?

Thus, our initial inquiry centers on unraveling the enigmatic role of *Singed* in BCM and exploring the possibility of its redundancy within this intricate genetic network. Through meticulous experimentation and genetic analyses, we aim to shed light on the underlying mechanisms governing BCM and the nuanced interactions among key genetic players, paving the way for a deeper understanding of developmental processes in *Drosophila* and beyond.

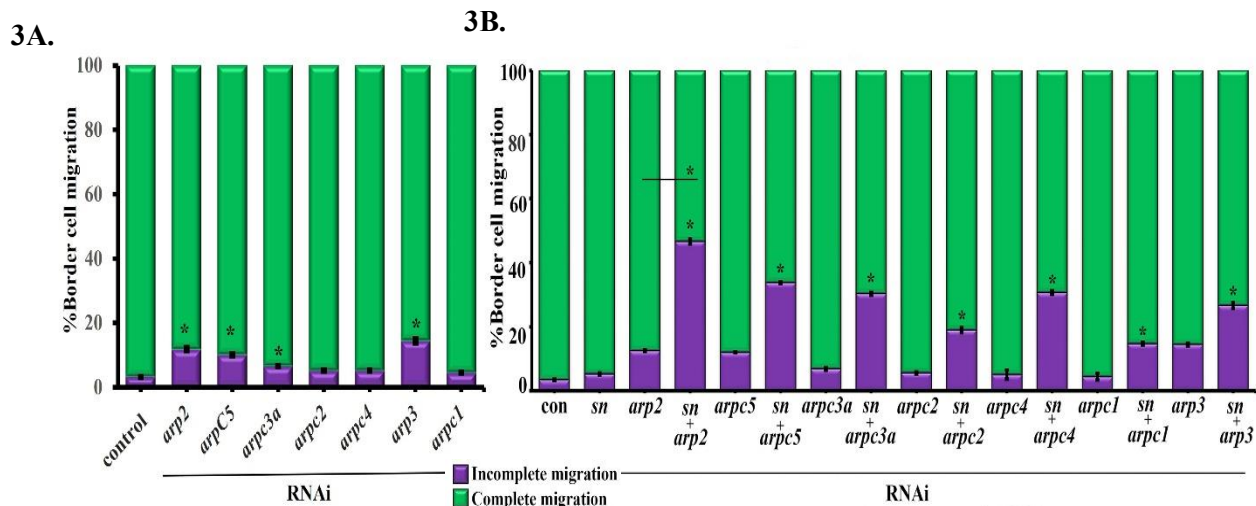


Fig 3. Genetic interaction between *singed* and *arp2/3* complex during border cell migration. 3A. represent effect of knockdown of *arp2/3* complex in border cells (n>300, R=3). 3B. represents interaction of *singed* with all the subunits of *arp2/3* complex (n>150, R=5). The disparities in means were found to be statistically significant (\*P ≤ .05) through both One Way ANOVA and t-tests. Error bars denote SEM.

We crossed *c306-GAL4*, *tubP-GAL80<sup>ts9</sup>* line with RNAi lines of *singed* and genes of Arp2/3 complex at 18°C, setting the stage for RNAi interaction studies in border cell migration (BCM). A critical initial step was to ascertain whether knocking down individual genes of each Arp2/3 complex subunit would indeed confer BCM defects. Our findings were striking – the knockdown of genes from each subunit resulted in noticeable BCM defects compared to the control, with the most significant defect observed when *arp3* was targeted (n>300, R=3) (Fig. 3A).

These compelling results unequivocally pointed towards the indispensable role of the Arp2/3 complex in governing BCM. Emboldened by these insights, we proceeded to unravel the intricate genetic interactions between *singed* and the Arp2/3 complex genes. The subsequent experiments were revealing – simultaneous knockdown of *singed* with individual subunits of the Arp2/3 complex led to a substantial impairment in BC migration.

In fact, this double knockdown often resulted in lethality, leading to a scarcity of adult females and stage 10 egg chambers in most cases. To mitigate this, we meticulously increased the number of replicates (R=5) to ensure an adequate sample size of stage 10 egg chambers (exceeding 150 samples).

Our meticulous analysis unearthed a statistically significant synergistic effect, particularly pronounced with *arp2*, where the migration defect soared to approximately 46% when combined with *singed* knockdown (see Fig. 3B for a visual depiction). These compelling observations provide strong evidence supporting the genetic interaction between *singed* and the Arp2/3 complex, hinting at a potential redundant role of *singed* in BCM.

This intriguing discovery opens up avenues for deeper exploration into the intricate genetic networks orchestrating BCM and sheds light on the dynamic interplay between key genetic players, paving the way for a comprehensive understanding of developmental processes in *Drosophila melanogaster*.

The intricate relationship between *Singed*, a parallel F-actin-bundling protein, and the Arp2/3 complex, a regulator of actin nucleation and branching, prompted us to delve deeper into their impact on the total F-actin levels within border cell (BC) clusters. Employing a rigorous approach, we quantified the F-actin levels using phalloidin staining in BC clusters via fixed imaging.

Our analysis revealed a significant reduction in F-actin levels upon single knockdown of either *Singed* or *Arp2*, with a more pronounced decrease observed in double knockdown clusters, compared to the control. This striking observation is vividly depicted in the box and whisker plot showcasing the mean phalloidin intensity of the clusters (refer to Fig. 4A for visualization).

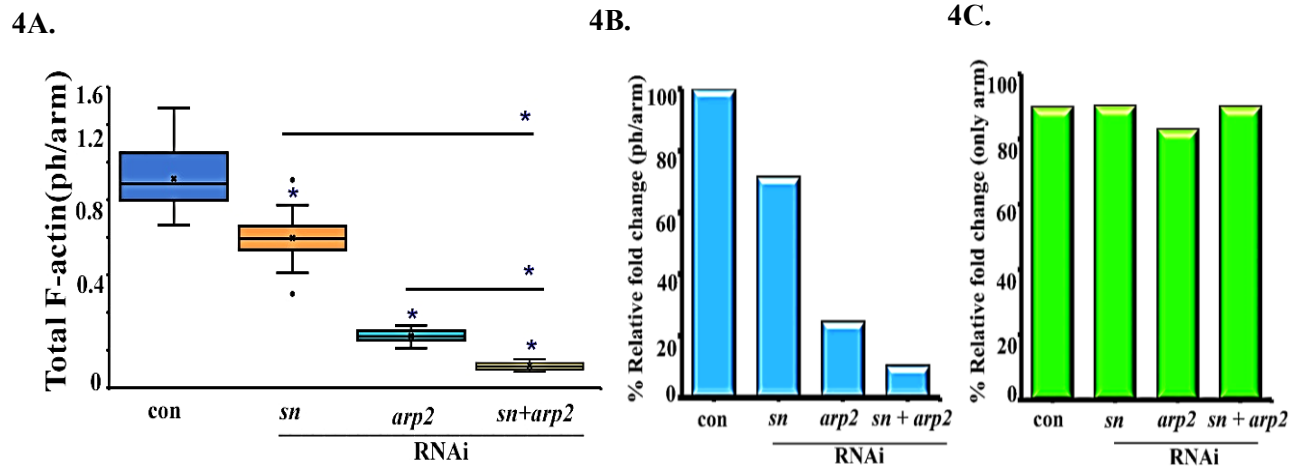


Fig4. *singed* and *arp2/3* complex regulates F-actin density in BCs during border cell migration.

4A. Box and whisker plots were utilized to depict the relative values of phalloidin over armadillo intensity, aiding in the determination of total F-actin via fixed imaging across indicated genotypes (n>50, R=3).

4B. Bar graph implying relative fold change of phalloidin/armadillo through fixed imaging in the denoted genotypes.

4C. The bar graph illustrates the relative fold change of the internal control armadillo across all specified genotypes.

Statistical analysis revealed significant differences in means ( $*P \leq .05$ ), as determined by One Way ANOVA. Error bars represent the standard error of the mean (SEM).

To ensure the robustness of our findings, we incorporated armadillo as an internal control and calculated the ratio of mean phalloidin intensity to mean armadillo intensity, providing a reliable measure for evaluating changes in F-actin levels. Notably, our data unveiled a 30% decrease in F-actin content in *Singed* knockdown clusters. However, this reduction was significantly amplified in *Arp2* knockdown clusters, showcasing a 70% decrease in F-actin content. Most strikingly, the double knockdown clusters exhibited a staggering 91% reduction in F-actin content, underscoring the synergistic impact of *Singed* and *Arp2* depletion on F-actin levels (refer to Fig. 4B for graphical representation).

Importantly, our analysis also included an examination of armadillo levels, serving as a control to ensure that changes in F-actin levels were not attributed to staining artifacts. Encouragingly, no significant changes in armadillo levels were observed in *Singed* knockdown, *Arp2* knockdown, or double knockdown clusters, affirming that alterations in

F-actin levels were indeed reflective of genuine biological changes (refer to Fig. 3C for visual depiction).

These are significant findings, which enhance our comprehension of the complex interactions among Singed, the Arp2/3 complex, and F-actin dynamics within BC clusters, shedding light on the underlying mechanisms governing border cell migration and

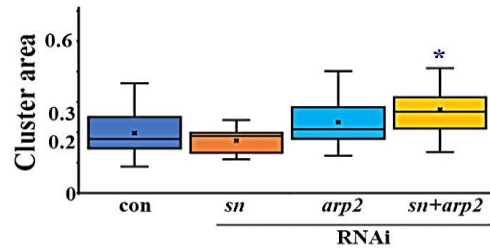
providing valuable insights for further exploration into cytoskeletal regulation during developmental processes.

During the BCM defect counting process as well as the imaging process, we observed that the BC clusters showed some interesting morphological characteristics and we decided to quantify them. Moreover, we decided to divide the observed characteristics into protrusion morphology and cluster shape.

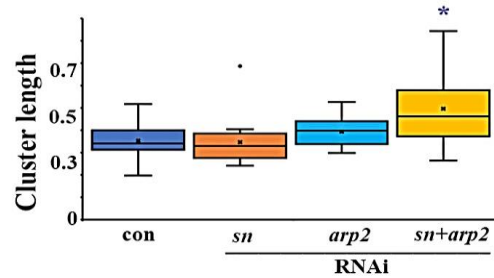
#### 4.1. Cluster shape from fixed imaging:

A captivating aspect of our investigation emerged when we delved into the morphological changes observed in double knockdown border cell (BC) clusters. Intriguingly, these clusters exhibited significant alterations in size and shape,

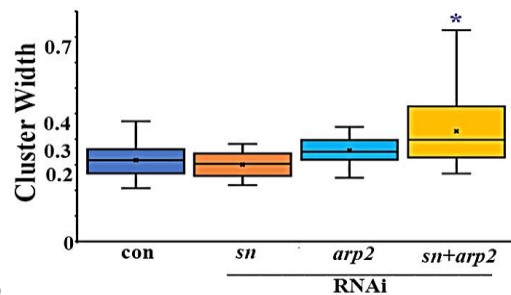
5A.



5B.



5C.



4D.

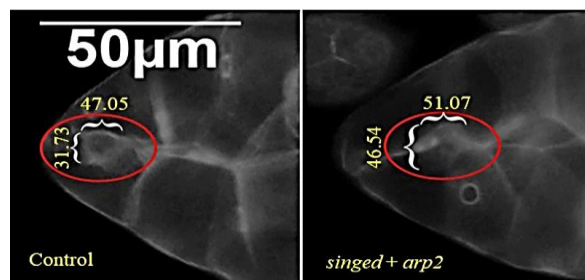


Fig. 5. *singed* and *arp2/3* complex affects border cell morphology in fixed samples. Box and Whisker plots representing border cell cluster area (5A), cluster length (5B) and cluster width (5C) through fixed imaging with indicated genotypes,  $n > 50$ .

(5D). Representative image showing relative F-actin density in fixed border cell cluster of control and double knockdown *sn+arp2* RNAi. The image also shows cluster width and length calculation. Scale 50  $\mu$ m.

Significant differences in means were observed ( $*P \leq .05$ ) through One Way ANOVA analysis. Error bars represent the SEM.

prompting us to embark on a meticulous analysis of their total cluster area using Fiji software, as illustrated in the box and whisker plots (refer to Fig. 5A for visual representation).

In our quest to understand these morphological transformations, we measured the area of BC clusters from fixed samples, focusing on those samples previously utilized for quantifying total F-actin levels (as depicted in Fig. 4A). The results were striking – a noteworthy increase in BC cluster area was observed specifically in the case of double knockdown samples, underscoring the influence of *Singed* and *Arp2* depletion on BC cluster morphology (refer to Fig. 5A for graphical representation).

However, in contrast, neither *Singed* knockdown nor *Arp2* knockdown alone exhibited any discernible changes in cluster size. This intriguing observation propelled us to delve deeper into the underlying mechanisms governing these alterations. Given that the cluster area is a composite measure of length and width, our curiosity led us to further dissect whether the observed changes were attributed to alterations in length, width, or both within double knockdown border cells.

Our analysis revealed a significant increase in both cluster length (refer to Fig. 5B) and width (refer to Fig. 5C) in fixed samples from the same batch used for area measurements, further reinforcing the notion that the morphological changes observed in double knockdown BC clusters are multifaceted and encompass alterations in both length and width.

The methods employed for these precise measurements are depicted in the accompanying image (refer to Fig. 5D), providing a comprehensive overview of our analytical approach.

### **For hs>FLP; AY-Gal4, UAS>Red stinger nls6/TM6B:**

After the hs>FLP; AY-Gal4, UAS>Red stinger nls6/TM6B flies were given heat shock, we saw red stinger being localized in few border cells. We then crossed the flies with *singed* and *arp2/3* complex to see whether it affects the border cells cluster. But we couldn't see

the red stinger localization (Fig. 7) in the nucleus of the BCs. However, we saw a good number of nucleus localization in the follicle cells. Further experiment is needed for this experiment to conclude anything regarding the interaction of *singed* and Arp2/3 complex.

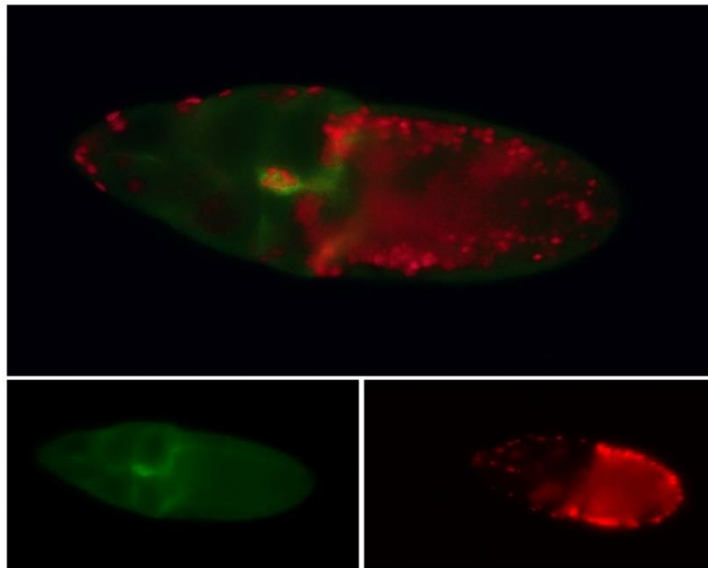


Fig. 6. Representative image for *hs>FLP; AY-Gal4, UAS>Red stinger nls6/TM6B*.

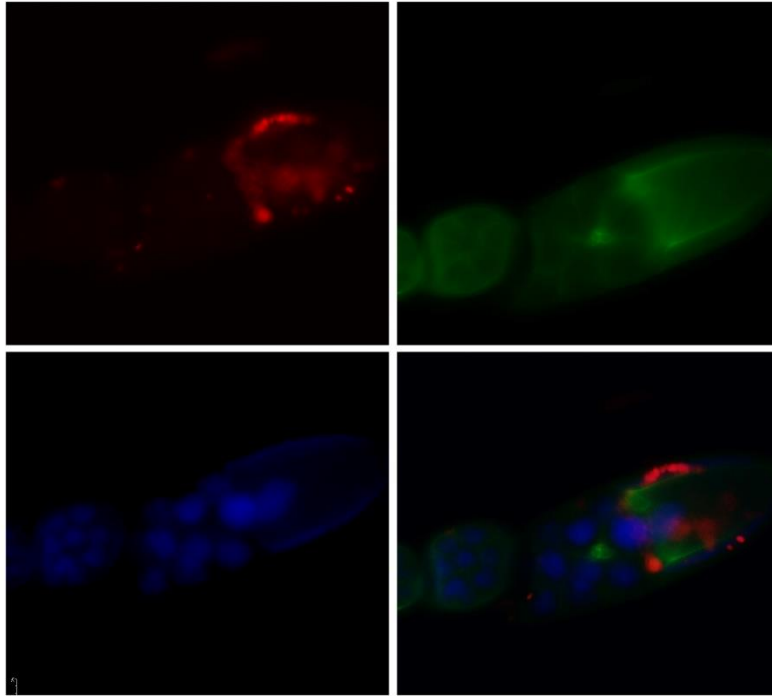


Fig. 7. Representative image of F1 flies for *hs>FLP/singed; AY-Gal4, UAS>Red stinger nls6/arp2* flies after HS.

## 5. Discussion:

In this work, we have tried to unravel the genetic interaction of another potent F-actin branching protein, the hetero-heptameric Arp2/3 complex, with *Singed* in regulating *Drosophila* BCM and therefore, *Singed* and Arp2/3 complex have become two crucial players in our work. Co-inhibition of *singed* with individual sub-unit of arp2/3 complex potentiates BCM defect significantly (Fig. 3B) which suggests synergistic interactions between the two, the maximum being with *arp2* followed by *arpC5*, *arpC4*, *arpC3A*, and *arp3* respectively (Fig. 3B). The vigor of this interaction during BCM can also be evidenced when both the gene affects cluster F-actin density and F-actin dependent characteristics. Significant reductions in total cortical F-actin level in the double knockdown clusters (Fig. 4A) have evidently proved that sparse F-actin density may have impeded considerable BCM defect. With increase in dissociation rate of cross-linkers, the

viscosity of actin filaments increases which make the cytoskeletal network more rigid, eventually impeding migration. We can assume that genetic knockdown of *singed* and *arp2* together may have reduced their binding ability with F-actin as less amount of Singed and Arp2 molecules were available, and their dissociation may have increased viscosity of the filaments of the migrating cluster (as F-actin density decreases) which may have hindered its migration. During CCM, the group of cells ought to create the force required to penetrate through the extracellular matrix (ECM) or other cells (nurse cells in the case of BCs). Therefore, from our data, it can be assumed that the drastic reduction of F-actin due to less amount of Singed and Arp2 molecules in double knockdown clusters has made them stiffer, viscous, and non-motile. We know that there is no ECM for BCs to adhere during migration. BC cluster ought to use the pull they get by adhering to the nurse cells and squeeze in between them on their route to the oocyte. Therefore, our data may suggest that when both are depleted, maximum stress has been given by nurse cells in their migratory pathway to hinder the migration of viscous and rigid BC clusters which can be another reason for the cluster to become stiff. <sup>[44]</sup> stated that actin-based structures having parallel crosslinkers exert less stress than those having actin-branching elements. Therefore, we might say that Singed-rich BC cluster employs less stress than Arp2/3 complex-rich cluster (also evident from their own migration defect Fig. 2B) and the stress increases during double knockdown. Moreover, we may also presume that maybe viscous and stiff BC clusters need greater surface area to withstand the stress conferred by nurse cells. Consequently, we can say that in rigid, viscous, and stiff clusters, less F-actin density may have not caused subtle protrusion dynamicity. Ultimately, we want to conclude that we have tried to present a better version of Singed protein, showing redundancy and Arp2/3 complex is its potential genetic partner. Moreover, we also assume that this regulation is a vigorous process with built-in redundancies.

Regarding the *hs>FLP; AY-Gal4, UAS>Red stinger nls6/TM6B* flies, the nucleus localization of cells is a very random process. In our result, we saw that there were quite a good number of follicle cells nucleus localization, but we couldn't see the same for BCs. Therefore, to comment on how they interact with *singed* and *arp2/3* complex is not very

clear. To unravel their interaction, we need to do the experiment more and see if there is any interaction.

### **5.1. Significance of the study:**

In double knockdown ones, the **cluster area** has increased compared to control. Thus, *singed* and *arp2/3* complex controls F-actin and F-actin-dependent characteristics in the BC cluster, which in the long run control BCM, thereby portraying redundancy of *singed* with *arp2/3* complex.

## **References:**

- 1) P.J. Keely, *Cell Migration within Three-Dimensional Matrices*, Encyclopedia of Biological Chemistry (2<sup>nd</sup> ed.), 2013, p. 436-445  
<https://doi.org/10.1016/B978-0-12-378630-2.00495-3>
- 2) Theveneau, E. and C. Linker, *Leaders in collective migration: are front cells really endowed with a particular set of skills?* F1000Res, 2017. 6: p. 1899.
- 3) Montell, D.J., W.H. Yoon, and M. Starz-Gaiano, *Group choreography: mechanisms orchestrating the collective movement of border cells*. Nat Rev Mol Cell Biol, 2012. **13**(10): p. 631-45
- 4) Wilson, K., et al., *Mechanisms of leading-edge protrusion in interstitial migration*. Nat Commun, 2013. 4: p. 2896.
- 5) Insall, R.H. and L.M. Machesky, *Actin dynamics at the leading edge: from simple machinery to complex networks*. Dev Cell, 2009. 17(3): p. 310-22
- 6) Meyen, D., et al., *Dynamic filopodia are required for chemokine-dependent intracellular polarization during guided cell migration in vivo*. Elife, 2015. 4.
- 7) Ribeiro, S.A., M.V. D'Ambrosio, and R.D. Vale, *Induction of focal adhesions and motility in Drosophila S2 cells*. Mol Biol Cell, 2014. 25(24): p. 3861-9.
- 8) Li, A., et al., *The actin-bundling protein fascin stabilizes actin in invadopodia and potentiates protrusive invasion*. Curr Biol, 2010. 20(4): p. 339-45.
- 9) Svitkina, T.M., *Ultrastructure of the actin cytoskeleton*. Curr Opin Cell Biol, 2018. 54: p. 1-8.
- 10) Verkhusha, V.V., S. Tsukita, and H. Oda, *Actin dynamics in lamellipodia of migrating border cells in the Drosophila ovary revealed by a GFP-actin fusion protein*. FEBS Lett, 1999. 445(2-3): p. 395-401.
- 11) Cant, K., et al., *Drosophila singed, a fascin homolog, is required for actin bundle formation during oogenesis and bristle extension*. J Cell Biol, 1994. 125(2): p. 369-80.
- 12) Breitsprecher, D. et al. (2011). *Molecular mechanism of Ena/VASP-mediated actin-filament elongation*. EMBO j. 30, 456–467.

- 13) Kurisu, S. and Takenawa, T. (2009). *The WASP and WAVE family proteins*. Genome Biol. 10, 226.
- 14) Alberts et al. *Molecular biology of the cell*. Fifth edition.
- 15) Chen, J., et al. (2001). *Cofilin/ADF is required for cell motility during Drosophila ovary development and oogenesis*. Nat Cell Biol, 3(2): p. 204-9
- 16) Volkmann, N. et al. (2001). *Structure of Arp2/3 complex in its activated state and in actin filament branch junctions*. Science. 293, 2456–2459
- 17) Robinson, R.C. et al. (2001). *Crystal structure of Arp2/3 complex*. Science 294, 1679–1684.
- 18) Gournier, H. et al. (2001). *Reconstitution of human Arp2/3 complex reveals critical roles of individual subunits in complex structure and activity*. Mol. Cell. 8, 1041–1052
- 19) Rouiller, I. et al. (2008). *The structural basis of actin filament branching by the Arp2/3 complex*. J. Cell Biol. 180, 887–895
- 20) Kelly, A.E. et al. (2006). *Actin binding to the central domain of WASP/Scar proteins plays a critical role in the activation of the Arp2/3 complex*. J. Biol. Chem. 281, 10589–10597.
- 21) Le Claire, L.L. et al. (2008). *Phosphorylation of the Arp2/3 complex is necessary to nucleate actin filaments*. J. Cell. Biol. 182, 647–654.
- 22) Krause, M. & Gautreau, A. (2014). *Steering cell migration: lamellipodium dynamics and the regulation of directional persistence*. Nat. Rev. Mol. Cell Biol. 15, 577–590.
- 23) Friedl, P. and D. Gilmour. (2009). *Collective cell migration in morphogenesis, regeneration and cancer*. Nat Rev Mol Cell Biol. 10(7): p. 445-57.
- 24) Svitkina, T.M. (2013). *Ultrastructure of protrusive actin filament arrays*. Curr Opin Cell Biol. 25(5): 574-81.
- 25) Sarmiento, C., Weigang Wang., W, Athanassios Dovas., A, Hideki Yamaguchi., H, Mazen Sidani., M., El-Sibai, M, DesMarais., V., Holman., HA., Kitchen., S., Backer., JB., Alberts., A., and John Condeelis., J. (2008). *WASP family*

- members and formin proteins coordinate regulation of cell protrusions in carcinoma cells.* The Journal of Cell Biology. 180, 1245–1260.
- 26) Hudson, AM and Cooley, L. (2002). *A subset of dynamic actin rearrangements in Drosophila requires the Arp2/3 complex.* J Cell Biol. 156(4): 677-687.
- 27) Svitkina, T.M., et al., (2003). *Mechanism of filopodia initiation by reorganization of a dendritic network.* J Cell Biol. 160(3): p. 409-21.
- 28) Leithner, A., Eichner, A., Muller, J., Reversat, A., Brown, M., Schwarz, J., Merrin, J., de Gorter, DJ., Schur, F., Bayerl, J. et al. (2016). *Diversified actin protrusions promote environmental exploration but are dispensable for locomotion of leukocytes.* Nat Cell Biol. 18:1253-1259.
- 29) Block, J. et al. (2012). *FMNL2 drives actin-based protrusion and migration downstream of Cdc42.* Curr. Biol. 22, 1005–1012.
- 30) Kage, F., Winterhoff, M., Dimchev, V., Mueller, J., Thalheim, T., Freise, A., Bruhmann, S., Kollasser, J., Block, J., Dimchev, G., Geyer, M., Schnittler, H., Brakebusch, C., et. al. (2017). *FMNL formins boost lamellipodial force generation.* Nature Communications. 8. 14832.
- 31) Aramaki S, Mayanagi K, Jin M, Aoyama K, Yasunaga T. (2016). *Filopodia formation by crosslinking of F-actin with fascin in two different binding manners.* Cytoskeleton (Hoboken). 73(7): 365-374.
- 32) Isogai, T. et al. (2015). *Initiation of lamellipodia and ruffles involves cooperation between mDia1 and the Arp2/3 complex.* J. Cell Sci. 128, 3796–3810.
- 33) Yang, C. et al. (2007). *Novel roles of formin mDia2 in lamellipodia and filopodia formation in motile cells.* PLoS Biol. 5, 317
- 34) Suetsugu, S. (2013). *Activation of nucleation promoting factors for directional actin filament elongation: Allosteric regulation and multimerization on the membrane.* Semin. Cell Dev. Biol. 24, 267-271.
- 35) Dayel, M. J., and Mullins, R. D. (2004). *Activation of Arp2/3 complex: addition of the first subunit of the new filament by a WASP protein triggers rapid ATP hydrolysis on Arp2.* PLoS Biol. 44, 56-59

- 36) Symons, M., Derry, J. M., Karlak, B., Jiang, S., Lemahieu, V., McCormick, F., Francke, U. and Abo, A. (1996). *Wiskott-Aldrich syndrome protein, a novel effector for the GTPase CDC42Hs, is implicated in actin polymerization*. Cell. 84, 723-734.
- 37) Majumder, P., Aranjuez, G., Amick, J., McDonald, J.A. (2012). *Par-1 controls Myosin activity and dynamics through Myosin Phosphatase to regulate border cell migration*. Curr Biol 22(5) 363-372.
- 38) Tamako Nishimura, Shoko Ito, Hiroko Saito, Sylvain Hiver, Kenta Shigetomi, Junichi Ikenouchi, Masatoshi Takeichi; *DAAM1 stabilizes epithelial junctions by restraining WAVE complex-dependent lateral membrane motility*. J Cell Biol 21 November 2016; 215 (4): 559–573.  
<https://doi.org/10.1083/jcb.201603107>
- 39) Fox, E. F., Lamb, M. C., Mellentine, S. Q., & Tootle, T. L. (2020). Prostaglandins regulate invasive, collective border cell migration. Molecular biology of the cell, 31(15), 1584–1594.  
<https://doi.org/10.1091/mbc.E19-10-0578>
- 40) Zhao, J., Cao, Y., DiPietro, L. A., & Liang, J. (2017). Dynamic cellular finite-element method for modelling large-scale cell migration and proliferation under the control of mechanical and biochemical cues: a study of re-epithelialization. Journal of the Royal Society, Interface, 14(129), 20160959.  
<https://doi.org/10.1098/rsif.2016.0959>
- 41) Narita, A., Mueller, J., Urban, E., Vinzenz, M., Small, J. V., & Maéda, Y. (2012). Direct determination of actin polarity in the cell. Journal of molecular biology, 419(5), 359–368. <https://doi.org/10.1016/j.jmb.2012.03.015>
- 42) Narita, A., Mueller, J., Urban, E., Vinzenz, M., Small, J. V., & Maéda, Y. (2012). Direct determination of actin polarity in the cell. Journal of molecular biology, 419(5), 359–368. <https://doi.org/10.1016/j.jmb.2012.03.015>